Electronic Supplementary Material (ESI) for Journal of Materials Chemistry A.

Supporting Information

highly ion conductive ion solvating membranes for durable alkaline water electrolysis at low temperature and voltage

*Bin Hu,[a,b] Zhongyan Li,[d] Lei Liu, *[c] Min Liu,[a,b] Yingda Huang,[a] Tiegen Guo,[e] Rong Zhang,[a,b] Kang Geng,*[a] and Nanwen Li, *[a,b,]*

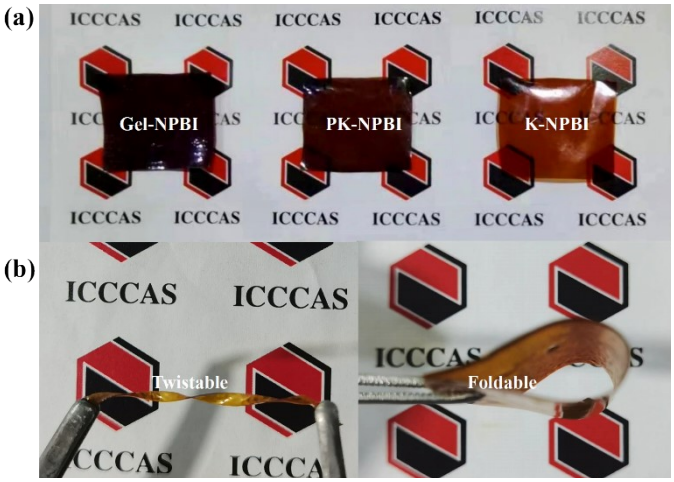

Figure S1. Digital photos of (a) three kinds of KOH doped NPBI membranes and (b) Gel-NPBI membrane be applied in twisting and folding.

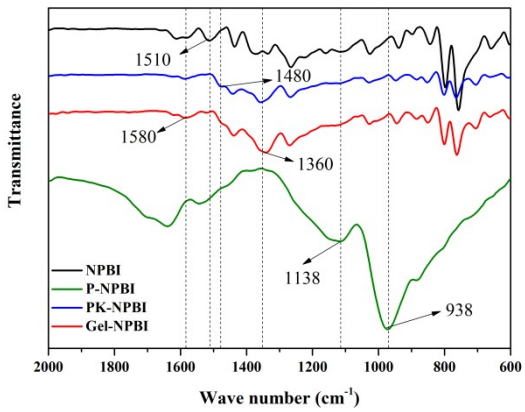

Figure S2. IR spectra of pristine NPBI membrane, and three NPBI-based ISMs in the region of 600 - 2000 cm^{-1}.

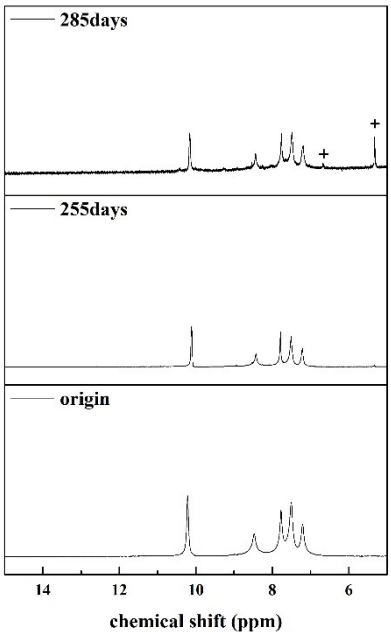

Figure S3. ^{1}H NMR spectra of pristine and aged PK-NPBI after immersion in 6M KOH at different durations.

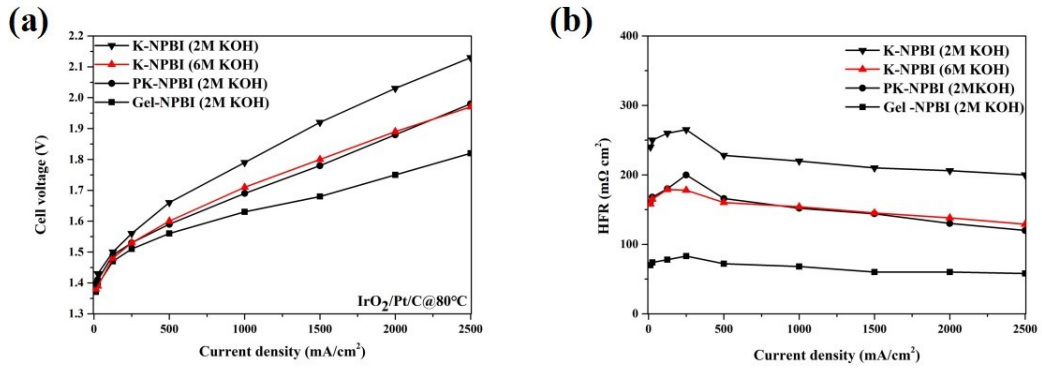

Figure S4. Comparison of electrolysis polarization (a) and high-frequency resistance (HFR) (b) in different KOH concentrations with different membranes: Gel-NPBI, PK-NPBI and K-NPBI membranes. Testing conditions: 80 ºC, 1.5 mg/cm^2 IrO_2 anode, and 0.5 mg/cm^2 Pt/C cathode.

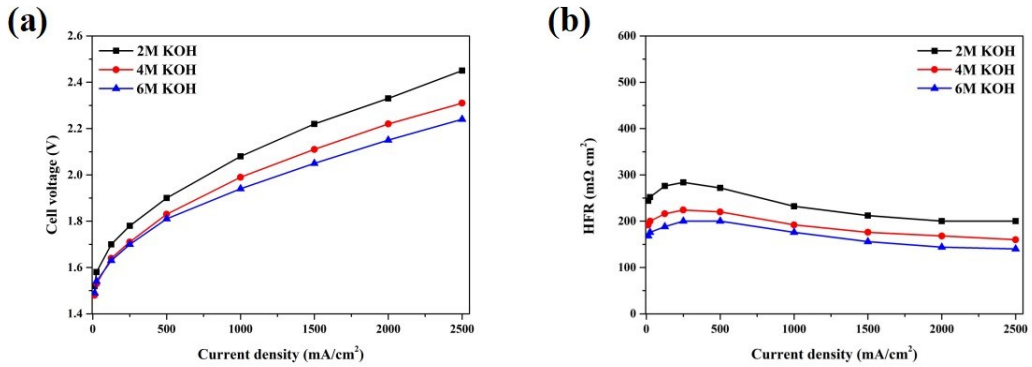

Figure S5. Comparison of electrolysis polarization (a) and high-frequency resistance (HFR) (b) consisting of different KOH concentrations with PK-NPBI membranes. Testing conditions: 80 ºC, anode/cathode with Ni/Al foam.

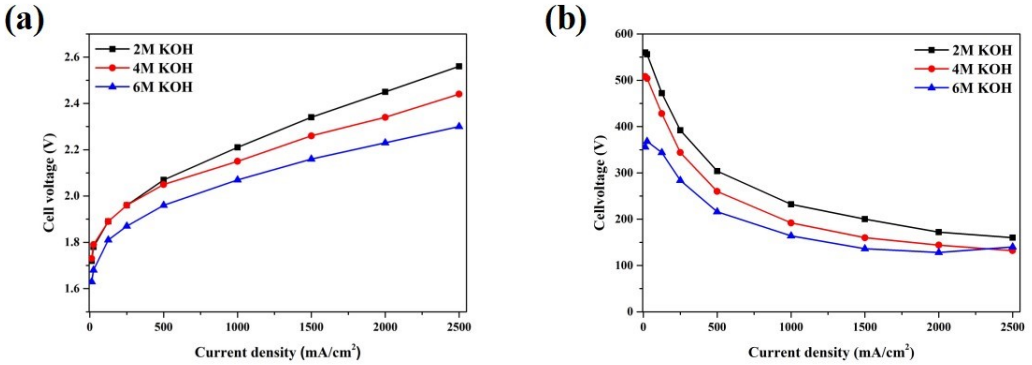

Figure S6. Comparison of electrolysis polarization (a) and high-frequency resistance (HFR) (b) consisting of different KOH concentrations with PK-NPBI membranes. Testing conditions: 80 ºC, anode/cathode with Ni foam.

	AEMS	Catalyst	Electrolyte	Temperature	Current density		Durability
21c	PTFE-Sustainions	Fe–Ni–Mo/Ni-Mo	1M KOH	80°C	1.57V	1A/cm^2	25h, 0.5A/cm^2, 1MKOH
1	PTFE-Sustainions	Ni–Fe	1 M KOH	60°C	2.0 V	0.62 A/cm^2	240h, 0.5A/cm^2, 60°C, 1MKOH
21a	PTFE-Sustainion	RANEY Ni $NiFe_2O_4$	1 M KOH	60°C	1.8V	0.84 A/cm^2	12000h, 1A/cm^2, 60°C, 1MKOH
21a	FAS-50	NiFeCo/$NiFe_2O_4$	1 M KOH	60°C	1.8 V	0.24 A/cm^2	200h, 1A/cm^2, 60°C
21b	A201	Ni/CP	1M KOH	50°C	1.9 V	0.35 A/cm^2	
21d	PBI/mTPN	Ni/Fe Mo	1M KOH	50°C	1.98V	0.25 A/cm^2	200h, 0.25A/cm^2, 50°C, 1MKOH
1	PFTP-13	Ni/Fe	1M KOH	80°C	2V	1.6 A/cm^2	1000h, 0.5A/cm^2, 60°C, 1MKOH
21i	Fumatech FAS-50	$NiFe_2O_4$ NiFeCo	1M KOH	60°C	1.9V	0.5 A/cm^2	200h, 1A/cm^2, 60°C, 1MKOH
21i	Sustainion 37-50	$NiFe_2O_4$ NiFeCo	1M KOH	60°C	1.9V	1 A/cm^2	2000h, 1A/cm^2,60°C,1MKOH
This work	**Gel-NPBI**	Pt/C@IrO_2	2M KOH	80°C	1.8V	2.5 A/cm^2	
This work	**Gel-NPBI**	Nickel/Al	6M KOH	80°C	1.9V	2 A/cm^2	1780h, 0.5A/cm^2, 58°C, 2MKOH
This work	**Gel-NPBI**	Nickel/Al	6M KOH	80°C	2.49V	8 A/cm^2	
This work	**Gel-NPBI**	Ni foam	6MKOH	80°C	2.2V	2 A/cm^2	
	ISMS	**Catalyst**	**Electrolyte**	**Temperature**	**Current density**		**Durability**
10	PTFE reforced Gel-mPBI	RANEY Ni	24% KOH	80°C	1.83V	1.8 A/cm^2	1000h, 0.5 A/cm^2, 80°C, 24% KOH
9a	m-PBI	RANEY Ni	24% KOH	80°C	1.8V	1.7 A/cm^2	
9a	m-PBI	Nickel foam	24%KOH	80°C	2.2V	1.2 A/cm^2	48h, 2V, 80°C, 20%KOH
9d	mes-PBI	Nickel foam	25% KOH	80°C	2.5V	1.1 A/cm^2	80h, 0.2A/cm^2, 80°C, 25%KOH
21h	Porous-PFSA		30% KOH	80°C	2.2V	0.2 A/cm^2	
9a	Zirfon	Nickel foam	30%KOH	80°C	2.3V	1 A/cm^2	
21g	Zirfon-80	Nickel foam	30%KOH	80°C	2V	1 A/cm^2	
21g	Zirfon-80	Nickel foam LDH-NiFe	30%KOH	80°C	2.1V	2 A/cm^2	300h, 1A/cm^2, 80°C 30%KOH
21e	NPBI-BS-47	Nickel foam	6M KOH	80°C	1.8V	1 A/cm^2	100h, 0.8/1.6A/cm^2, 80°C, 6MKOH
36	PVA-ABPBI	Nickel foam	15%KOH	70°C	1.9V	0.36 A/cm^2	60min, 0.2A/cm^2, 70°C, 15%KOH
21f	PF41	Nickel foam	20%KOH	60°C	2.2V	0.4 A/cm^2	100h, 0.2A/cm^2, 60°C, 20%KOH

Table S1. Comparison of the state-of-the-art AEMWEs with PGM-free catalysts in current research.

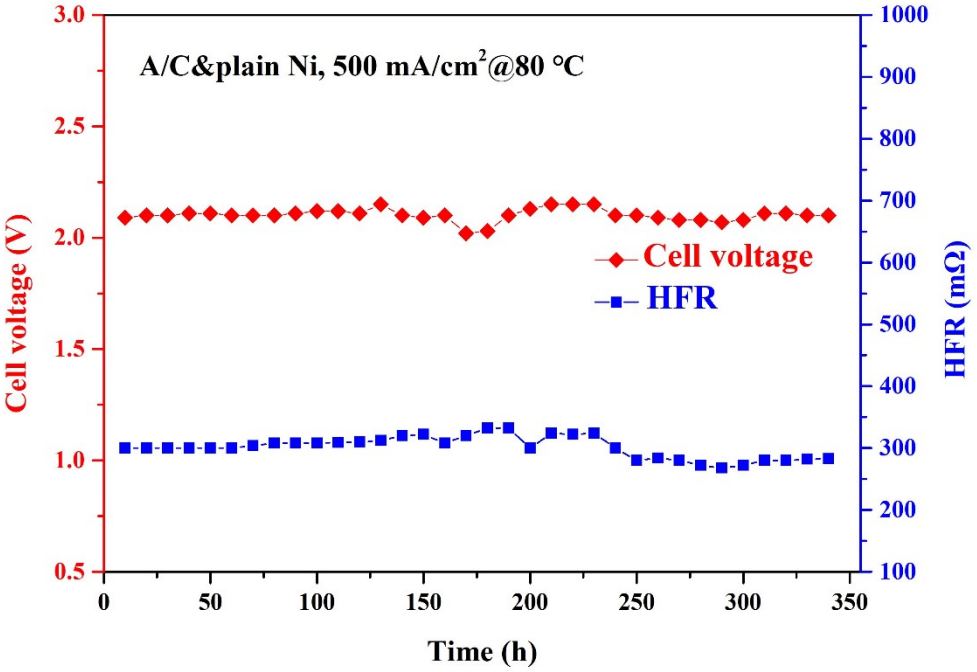

Figure S7. In-situ durability of A/C Ni–Al AEMWE based on the PK-NPBI membrane in 2M KOH under 0.5 A/cm^2 at 80ºC

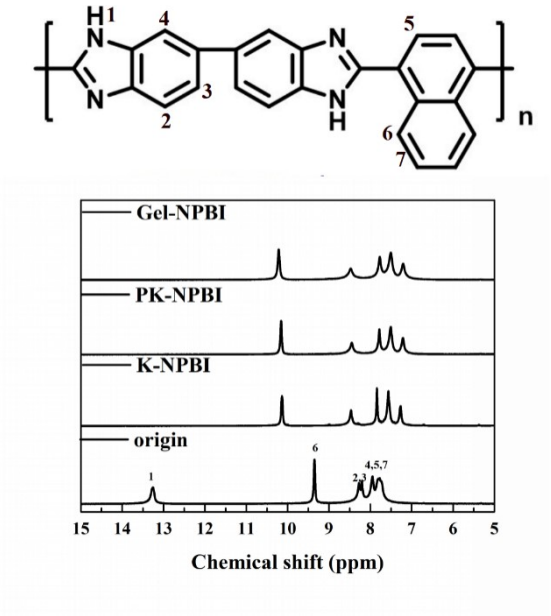

Figure S8. 1H NMR spectra of homogeneous and Gel-NPBI membrane.

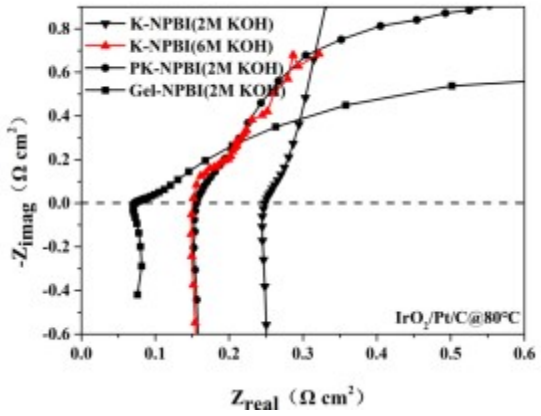

Fig.S9 Impedance curves at 250 mA/cm^2, Operating conditions: 80 ºC, 1.5 mg/cm^2 IrO_2 anode, and 0.5 mg/cm^2 Pt/C cathode

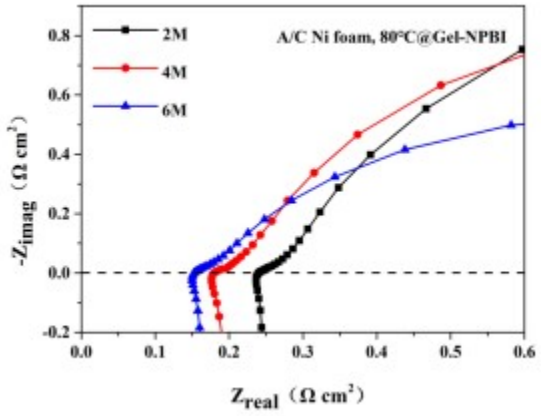

Fig.S10 Impedance curves at 250 mA/cm^2, Operating conditions: 80 ºC, anode/cathode with Ni foam

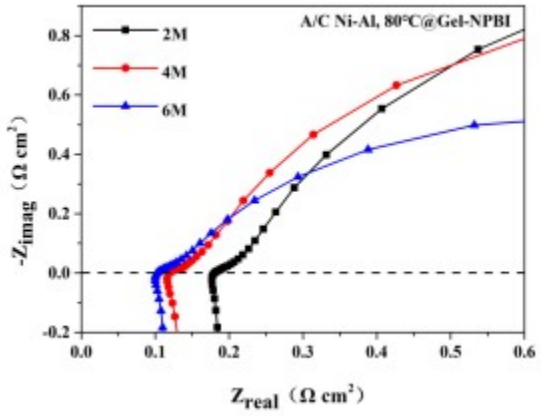

Fig.S11 Impedance curves at 250 mA/cm^2, Operating conditions: 80 ºC, anode/cathode with Ni/Al foam

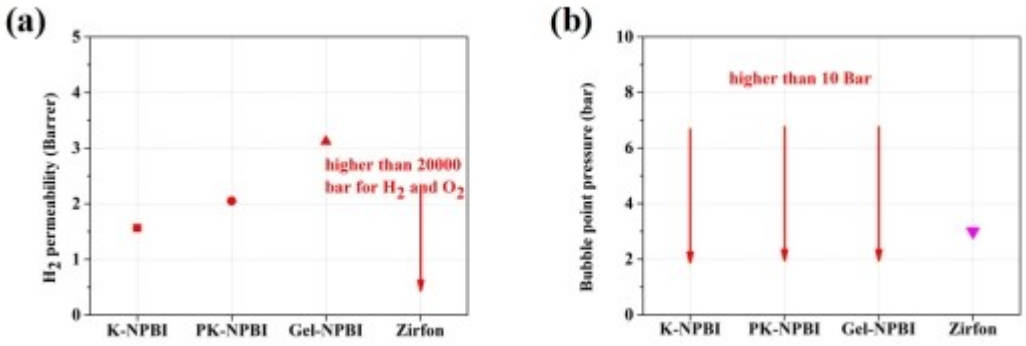

Fig.S12. The H_2 permeability (a) and bubble point pressure (b) of K-NPBI, PK-NPBI, Gel-NPBI, and Zirfon at room temperature

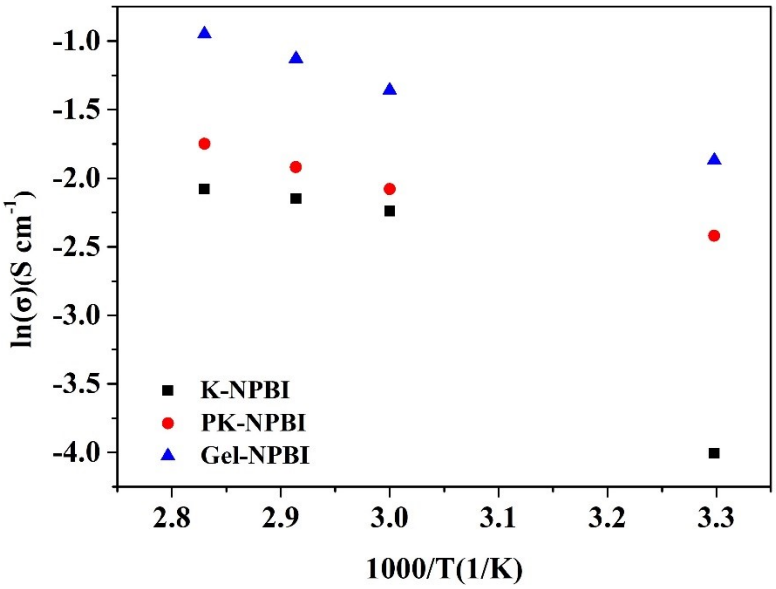

Fig. S13 the relationship between ln(σ) and 1000/T for different membrane in 6 M KOH.

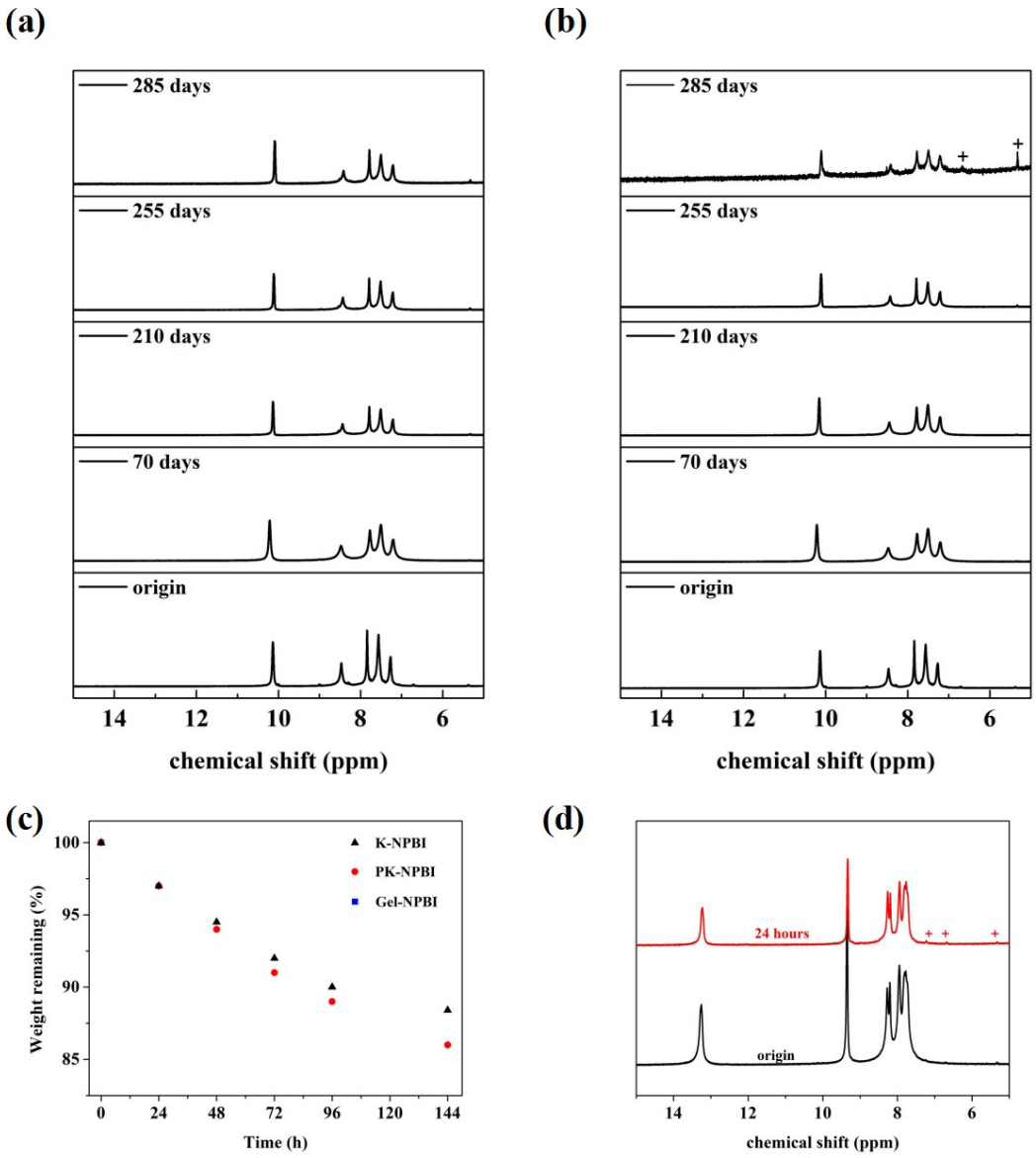

Fig.S14 ^{1}H NMR spectra of origin and aged Gel NPBI after immersion in (a) 2M and (b) 6M KOH at different durations; (c) Weight change of dry membranes in Fenton's reagent at 80 ºC for different durations and (e) ^{1}H NMR spectra of Gel-NPBI membrane in DMSO-d6 before and after oxidation test.

intrinsic viscosity	Test condition	Initial	After In situ tests
Gel-NPBI	(2M 80℃ 2 V)	1.63	0.84
Gel-NPBI	(6M 80℃ 1.95 V)		0.65
Gel-NPBI	(2M 30℃ 2.75 V)		0.42
Gel-NPBI	(2M 30℃ 2.2 V)		1.09
Gel-NPBI	(2M 58℃ 2.15V)		1.2
Gel-NPBI	(6M 58℃ 2.1V)		0.97

Table S2 Intrinsic viscosities for Gel-NPBI membranes before and after in situ durability tests at different conditions

H_2 permeability(barrer)	Initial	After In situ tests
Gel-NPBI[a]	3.54	4.7
Gel-NPBI[b]	3.52	6.97

Table S3 gas permeability of Gel-NPBI before and after durability test at 58 ℃

Testing conditions: [a] the cell durability was tested at 500 mA cm^{-2} and 58 ºC using 2 M KOH electrolyte; [b] the cell durability was tested at 500 mA cm^{-2} and 58 ºC using 6 M KOH electrolyte.

Reference

[1] a)N. Chen, S. Y. Paek, J. Y. Lee, J. H. Park, S. Y. Lee, Y. M. Lee, *Energy & Environmental Science* 2021, *14*, 6338-6348.

[9] a)M. R. Kraglund, M. Carmo, G. Schiller, S. A. Ansar, D. Aili, E. Christensen, J. O. Jensen, *Energy & Environmental Science* 2019, *12*, 3313-3318; d)D. Aili, A. G. Wright, M. R. Kraglund, K. Jankova, S. Holdcroft, J. O. Jensen, *Journal of Materials Chemistry A* 2017, *5*, 5055-5066.

[10] M. L. A. Trisno, A. Dayan, S. J. Lee, F. Egert, M. Gerle, M. R. Kraglund, J. O. Jensen, D. Aili, A. Roznowska, A. Michalak, H. S. Park, F. Razmjooei, S.-A. Ansar, D. Henkensmeier, *Energy & Environmental Science* 2022, *15*, 4362-4375.

[21] a)B. Motealleh, Z. Liu, R. I. Masel, J. P. Sculley, Z. R. Ni, L. Meroueh, *International Journal of Hydrogen Energy* 2021, *46*, 3379-3386; b)L. A. Diaz, R. E. Coppola, G. C. Abuin, R. Escudero-Cid, D. Herranz, P. Ocon, *Journal of Membrane Science* 2017, *535*, 45-55; c)P. Chen, X. Hu, *Advanced Energy Materials* 2020, *10*; d)M. Najibah, E. Tsoy, H. Khalid, Y. Chen, Q. Li, C. Bae, J. Hnat, M. Plevova, K. Bouzek, J. H. Jang, H. S. Park, D. Henkensmeier, *Journal of Membrane Science* 2021, *640*; e)X. Hu, M. Liu, Y. Huang, L. Liu, N. Li, *Journal of Membrane Science* 2022, *663*; f)A. Konovalova, H. Kim, S. Kim, A. Lim, H. S. Park, M. R. Kraglund, D. Aili, J. H. Jang, H.-J. Kim, D. Henkensmeier, *Journal of Membrane Science* 2018, *564*, 653-662; g)H. I. Lee, M. Mehdi, S. K. Kim, H. S. Cho, M. J. Kim, W. C. Cho, Y. W. Rhee, C. H. Kim, *Journal of Membrane Science* 2020, *616*; h)D. Aili, M. K. Hansen, J. W. Andreasen, J.

Zhang, J. O. Jensen, N. J. Bjerrum, Q. Li, *Journal of Membrane Science* 2015, *493*, 589-598; i)Z. Liu, S. D. Sajjad, Y. Gao, H. Yang, J. J. Kaczur, R. I. Masel, *International Journal of Hydrogen Energy* 2017, *42*, 29661-29665.